Radiation Measurements 50 (2013) 61–66

Contents lists available at SciVerse ScienceDirect

Radiation Measurements

journal homepage: www.elsevier.com/locate/radmeas

Characterization of the neutron field from the ^{241}Am-Be isotopic source of the IPHC irradiator

K. Amgarou [a,*], M. Trocmé [b], M.J. García-Fusté [a], M. Vanstalle [b], E. Baussan [b], A. Nourreddine [b], C. Domingo [a]

[a] Grup de Recerca en Radiacions Ionitzants (GRRI), Departament de Física, Universitat Autònoma de Barcelona, E-08193 Bellaterra, Spain
[b] Groupe de Radioprotection et Mesures Environnementales (RAMSES), Institut Pluridisciplinaire Hubert-Curien (IPHC), UMR 7178 CNRS-UN2P3/ULP, 23 rue de Loess, F-67037 Strasbourg Cedex 2, France

HIGHLIGHTS

► We describe a neutron irradiation facility based on ^{241}Am-Be radioactive source.
► The neutron field was characterized with a Bonner sphere spectrometer (BSS).
► Monte Carlo simulations using the MCNPX code were in good agreement with BSS.
► The un-scattered neutron spectrum is provided and compared to that given by the ISO-8529 standard.
► The neutron intensity of the ^{241}Am-Be source is also estimated.

ARTICLE INFO

Article history:
Received 16 December 2011
Received in revised form
8 November 2012
Accepted 16 November 2012

Keywords:
Neutron irradiation facility
^{241}Am-Be source
Bonner sphere spectrometer

ABSTRACT

A measurement campaign has been carried out recently to provide the source intensity and the reference spectra around a neutron irradiation facility based on ^{241}Am-Be radionuclide source, using the UAB Bonner Sphere Spectrometer. This facility, which consists of a bunker, a container/shielding for the source and an irradiation device that uses an automated remote-controlled system for the source positioning and rotating during the dosimeter irradiation, is intended to be routinely used to check the response of passive dosimeters, namely those based on photo-stimulated imaging plates and solid-state nuclear track detectors. The measurement results, in terms of neutron spectra and global dosimetric quantities (i.e., fluence and ambient dose equivalent rates) at different distances with respect to the ^{241}Am-Be source, were compared with Monte Carlo simulations using the MCNPX code and a good agreement was observed. An estimation of the un-scattered neutron spectrum directly emitted from the ^{241}Am-Be source is given as well.

1. Introduction

The French RAMSES (*Radioprotection et Mesures Environnementales*) group of the IPHC (*Institut Pluridisciplinaire Hubert-Curien*, Strasbourg) centre develops its research activities in the field of radiation protection and offers expertise services in the environmental radioactivity (natural or artificial) measurements (Dziri et al., 2012; Abou-Khalil et al., 2009; Ouziane et al., 2010; Ngachin et al., 2008). The group is currently accredited for external personal dosimetry of workers professionally exposed to ionizing radiation and participates in their initial formation and on-going training. To routinely check the response of the passive dosimeters, namely those based on photo-stimulated imaging plates (Mouhssine et al., 2005) and solid-state nuclear track detectors (Fernández et al., 2005), a neutron irradiation facility, using an ^{241}Am-Be radionuclide source, was set-up in 2008. An automated remote-controlled system is used for the source positioning and rotation during the dosimeter irradiation.

This work reports on the description of this irradiation facility as well as on a measurement campaign carried out recently by the Spanish GRRI (*Grup de Recerca en Radiacions Ionitzants*) group of the *Universitat Autònoma de Barcelona* (UAB), in the framework of a research collaboration. The aim of this campaign is to provide the source intensity and the neutron spectra at different locations within the bunker by means of a Bonner sphere spectrometer (BSS). This

* Corresponding author. Tel.: +34 93 581 1364; fax: +34 93 581 2155.
E-mail addresses: khalil.amgarou@uab.cat (K. Amgarou), carles.domingo@uab.cat (C. Domingo).

1350-4487/$ – see front matter © 2012 Elsevier Ltd. All rights reserved.
http://dx.doi.org/10.1016/j.radmeas.2012.11.015

measuring system, firstly introduced by Bramblett et al. in (1960), consists of a set of polyethylene moderating spheres of various sizes with a central detector mainly sensitive to thermal neutrons. The angular response of the BSS shows a very small dependence on the neutron direction of incidence (Fernández et al., 2007a). Its fluence response extends over a wide energy range (from thermal up to a few tens MeV and can be extended to several hundreds MeV by inserting shells of materials with high atomic mass). The unique drawback of a BSS is its limited energy resolution that does not allow appreciating detailed structures such as oscillations and resonances on the measured neutron spectrum. Therefore, only smooth distributions of possible neutron fluence peaks could be indicated by this system. Even with this limitation, the UAB-BSS (Bakali, 2001), which was extensively validated in reference quasi mono-energetic beams as well as in radionuclide based sources and the thermal SIGMA facility at IRSN (Cadarache, France) (Lacoste et al., 2004; Bedogni et al., 2010), has shown its convenience to characterize the neutron fields in several workplace environments (Amgarou et al., 2011; Bedogni et al., 2007a; Esposito et al., 2010; Domingo et al., 2009; Fernández et al., 2004, 2007b, 2007c; Gressier et al., 2004).

2. Material and methods

2.1. Neutron irradiation facility

The IPHC neutron irradiation facility is located in a small concrete bunker (see Fig. 1) and consists of a polyethylene (PE) cube ($84 \times 84 \times 84$ cm^3), located at the centre of the bunker floor, with a central Al tube through which the ^{241}Am-Be source, with a nominal activity of 3.7×10^{10} Bq (1 Ci), can be extracted by means of an automated system. This system consists of a motor-driven screw that can go up and down within the Al tube, and that can be also used to rotate the source during the irradiation to avoid irradiation irregularities due to the effects of possible source inhomogeneity. The vertical source irradiation position is about 44 cm above the PE cube at 128 cm from the room floor. Two Al arms on opposite sides of the PE cube are used as supports and in one of them the source-detector distance can be adjusted automatically. At the end of irradiation, the ^{241}Am-Be source is stored in the centre of the PE cube that absorbs almost all the emitted neutrons. The bunker, which is accessed by a maze entrance, has a main space of approximately $404 \times 413 \times 386$ cm^3 surrounded with lateral walls 1 m in thickness. All the irradiator controls can be done remotely, from outside the bunker, to avoid any unnecessary risk of exposure for the user.

2.2. Bonner sphere spectrometer

The UAB-BSS measuring system is based on a cylindrical (10 mm diameter and 9 mm high) ^{3}He filled (8 kPa) proportional counter (model 05NH1 from EURISYS) that is normally introduced in the centre of 8 PE (100% purity and 0.920 ± 0.003 g cm^{-3} density) spheres, whose diameters are labelled in inch units (2.5 in., 3 in., 4.2 in, 5 in., 6 in., 8 in., 10 in., 12 in.) for convenience. In addition, a 1 mm thick cadmium (Cd) cover may be used for the 3 smallest spheres to accurately derive the thermal component (below 0.5 eV) of the neutron spectra. Since this spectrometer shows an inherent upper limit at 20 MeV (above this energy the cross-section of the n-p elastic scatterings drops off significantly), two extended range spheres, with Cu and Pb inserts, were added recently (Esposito et al., 2010) to measure also neutrons with energies up to several hundreds of MeV. One of these new high-energy spheres (7 in. + Cu) consists on an internal PE sphere 3 in. in diameter, covered with a Cu shell 1 in. in thickness, adjacent to an external PE layer 1 in. in thickness. The other extended-range sphere (7 in. + Pb) is similar, hosting a lead shell 1 in. in thickness.

The response matrix of the UAB-BSS was calculated, using MCNPX (Waters, 2002), for 121 logarithmic equidistant discrete neutron energy values ranging from 7.943×10^{-4} eV up to 1.259 GeV. As already stated in Section 1, the matrix was validated in reference quasi mono-energetic beams at PTB (Braunschweig, Germany) and JRC-IRMM (Geel, Belgium) as well as in radionuclide based sources and the thermal SIGMA facility at IRSN (Cadarache, France) (Lacoste et al., 2004; Bedogni et al., 2010), providing an overall uncertainty of $\pm$3%. The spectrometer calibration was verified in March 2008 using the INFN ^{241}Am-Be source and in February 2010 with the NPL ^{252}Cf source, and its calibration factor was confirmed within 2%.

The extended-range spheres were not used, since the neutron spectrum form an Am-Be source extends up to about 10 MeV. Because of the small dimension of the bunker, five points at distances 75, 110, 145, 180 and 215 cm from the ^{241}Am-Be source, along the diagonal direction of the bunker and at the same vertical position of the source (128 cm from the room floor) were selected for measurements. The last point was already very close to the room corner, at practically 50 cm from the two adjacent lateral walls.

2.3. Full count rates, un-scattered and scattered components and source intensity

The source neutron yield and energy distribution (spectrum) may be obtained from the readings at the measurement points, taking into account room scattering and, eventually, air attenuation. According to the ISO-8529 standard, it can be assumed that the *scattered component* is uniform in a finite irradiation room (constant scattering approximation), whereas the *direct component* follows exactly the $1/d^2$ law. As the dimensions of the room are small, air-attenuation can be neglected. Linear fits of the *full* count rates c_d^i vs. $1/d^2$ were performed for the readings obtained at the 5 measurement points with the 11 sphere configurations of our Bonner spectrometer. If there were no room scattering, the intercept

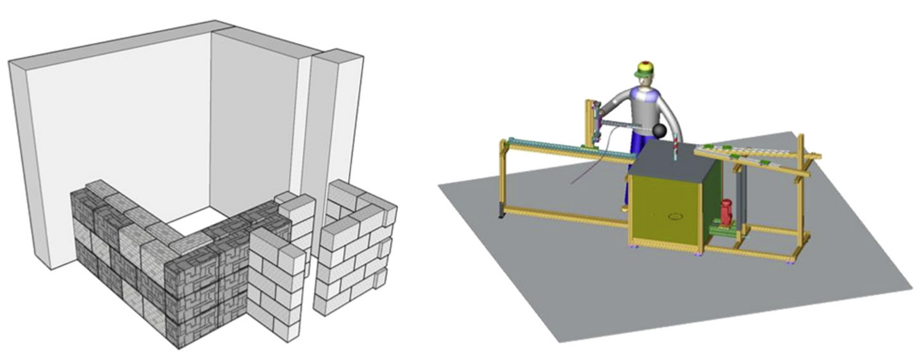

Fig. 1. A simple sketch of the IPHC neutron irradiation facility.

of this straight line would be 0 (the expected count rate for $1/d^2 = 0$, i.e., $d = \infty$). In the constant scattering approximation, this intercept, c^i_∞, gives the count rate for the specified sphere i due to the *scattered* component. By subtracting this value from the *full* count rate c^i_d, the count rate $C^i_d = c^i_d - c^i_\infty$ due to the *direct* (un-scattered) component can be obtained for the sphere i at distance d. By using the exact $1/d^2$ law, the count rate C^i_{REF} for sphere i due to the *direct* component may now be evaluated for any arbitrary reference distance d_{REF}. In our case d_{REF} was set to 1 m.

The unfolding code FRUIT (Bedogni et al., 2007b) was especially designed as a tool for operational measurements in scenarios where very scarce pre-information is available. FRUIT makes use of the so called "*parametric approach*", modelling the neutron spectrum as a superposition of elementary functions, covering the different energy domains and fully described by a reduced number (less than ten) of physically meaningful parameters. This approach, also used in the Bayesian methods (Reginatto, 2010), avoids the necessity of providing a *guess* spectrum, typically derived from Monte Carlo simulations and preferably very similar to the spectrum to be determined. FRUIT only requires introducing qualitative information on the type of "*radiation environment*" in a check-box input section. The code randomly generates a default spectrum, needed to start the iterative procedure, based on the radiation environment selected by the user. Taking advantage of a "*flexible tolerance*" convergence mechanism, results do not depend on the numerical values of this spectrum.

Full neutron spectra $\Phi_{E,d}(E) = \mathrm{d}\Phi/\mathrm{d}E$ and fluence rates $\dot{\Phi}_d$, as experienced by a detector located at the measurement points in the bunker, were obtained by unfolding with FRUIT the *full* count rates c^i_d acquired with the UAB-BSS. The spectrum of the *direct* neutron component (source spectrum) and the *direct* (or un-scattered) neutron fluence rate $\dot{\Phi}^u_{\mathrm{REF}}$ at d_{REF} are evaluated by unfolding the C^i_{REF} counts. The neutron source yield or intensity I is therefore calculated as $I = 4\pi d^2_{\mathrm{REF}} \dot{\Phi}^u_{\mathrm{REF}}$. Ambient dose equivalent rates $\dot{H}^*_d$ were obtained by folding the neutron spectrum at the considered point with the fluence-to-ambient dose equivalent conversion coefficients recommended by the ICRP-74 (ICRP, 1997).

2.4. Monte Carlo simulation

The MCNPX radiation transport code was used for the theoretical characterization of the neutron field at the IPHC irradiation facility. The geometry described in Section 2.1 was strictly specified in the input file of the simulation code. An isotropic ^{241}Am-Be source with the energy distribution taken form the ISO-8529 standard (ISO, 1989) was detailed. The inner space of the experimental hall was filled with dry air; whereas its lateral walls and floor were assumed to be made of ordinary concrete (density 2.4 g cm^{-3}). Information about the interactions of neutrons, photons and protons with the material components was extracted from the evaluated nuclear library, ENDF/B-VI release 8. In addition, $S(\alpha,\beta)$ treatment option was used to account for the carbon and hydrogen chemical binding

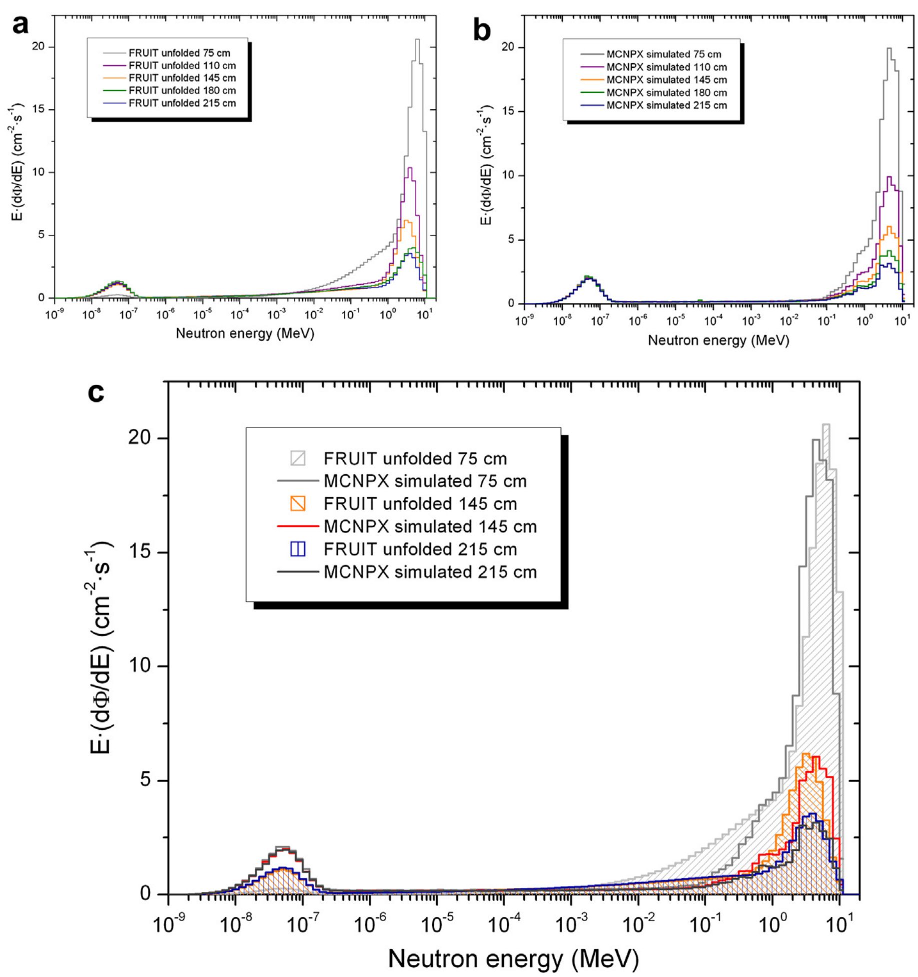

Fig. 2. (a) Neutron spectra at each measurement point obtained by unfolding with FRUIT the row Bonner sphere measurements; (b) Neutron spectra at each measurement point computed using MCNPX; (c) Comparison of the unfolded and simulated neutron spectra at three representative points (d = 75 cm, 145 cm and 215 cm).

at room temperature during thermal neutron scattering within the PE cube. The neutron energy distributions at each point of interest were obtained by means of the point detector (F5) tally. A total of 104 logarithmic equidistant energy bins (i.e., ten per decade) between 10^{-9} and 20 MeV were chosen for the output spectra. The number of histories was large enough to have individual uncertainties below 5% in each energy bin.

Note that all MCNPX simulation output results (neutron energy spectrum and total fluence rate) are evaluated per unit emitted neutron. It is therefore necessary to multiply these results by the measured neutron source intensity I, obtained as described in 2.3, in order to make correct estimations of the absolute value of simulated fluence rates or to present absolute neutron spectra at a given point.

3. Results and discussion

Full neutron spectra and total fluence rates $\dot{\Phi}_d$ at each measurement point were obtained by unfolding with FRUIT the corresponding row count rates c_d^i, as described in 2.3. The lethargy plots ($E\,d\Phi/dE$ against E in logarithmic scale) of the unfolded spectra are presented in Fig. 2a, while Fig. 2b displays the spectra simulated with MCNPX at the same points. Comparison between simulated and unfolded spectra is shown in Fig. 2c for three representative points ($d = 75$ cm, 145 cm and 215 cm). The total fluence rate values $\dot{\Phi}_d$ and ambient dose equivalent rates $\dot{H}_d^*(10)$ obtained from unfolding with FRUIT and from MCNPX Monte Carlo calculation are displayed in Table 1. All together, a good agreement between the UAB-BSS measurements and MCNPX simulations is achieved. Fig. 3a displays the fits of count rates against $1/d^2$ for some representative spheres (2.5″ + Cd, 4.2″, 5″, 6″, 8″ and 12″) and Fig. 3b shows the plot of $\dot{\Phi}_d$ against $1/d^2$. Least squares fit leads to an intercept value $\dot{\Phi}_\infty = (9.60 \pm 0.36)$ cm^{-2} s^{-1}, which may be understood as a rough estimation of the scattered fluence rate value. As the direct component is comprised basically of fast neutrons (from 10 keV to 1 MeV) and the scattered component includes epithermal and thermal neutrons, it can be assessed that the fast neutron component (from 10 keV to 1 MeV) decreases with distance (d) according to the $1/d^2$ law, while the epithermal and thermal components, originated all over the concrete lateral walls and floor, as well as in the PE cube, remain approximately uniform throughout the irradiation room.

The procedure described in Subsection 2.3 was applied for deriving the direct and the scattered components. Firstly, the expected count rates due to the scattered component for each sphere, c_∞^i, were estimated. Secondly, the count rates, C_d^i, due to the direct component were calculated for each sphere i at all distances d where measurements were made. Finally, the count rates C_{REF}^i due to the direct component at $d_{\mathrm{REF}} = 1$ m for all spheres i were evaluated by using the exact $1/d^2$ law. Unfolding C_{REF}^i with FRUIT, we obtained the spectrum of the un-scattered component and its fluence rate at d_{REF}, $\dot{\Phi}_{\mathrm{REF}}^u = (17.82 \pm 0.98)$ cm^{-2} s^{-1}. The resulting source intensity is therefore $I = 4\pi d_{\mathrm{REF}}^2 \dot{\Phi}_{\mathrm{REF}}^u = (2.24 \pm 0.12) \times 10^6$ s^{-1}. Uncertainties

Table 1
Measured and MCNPX computed neutron fluence and ambient dose equivalent rates at every measurement point.

Distance	Φ (cm^{-2} s^{-1})		$H^*(10)$ (μSv h^{-1})	
	UAB-BSS	MCNPX	UAB-BSS	MCNPX
75 cm	41.0 ± 1.9	40.8 ± 1.8	48.8 ± 2.4	49.9 ± 2.5
110 cm	23.6 ± 1.1	24.2 ± 1.1	25.3 ± 1.3	24.5 ± 1.2
145 cm	17.2 ± 0.8	17.7 ± 0.8	16.3 ± 0.7	16.2 ± 0.7
180 cm	15.3 ± 0.7	14.7 ± 0.7	12.0 ± 0.6	12.7 ± 0.6
215 cm	13.5 ± 0.6	13.0 ± 0.6	9.6 ± 0.4	10.4 ± 0.5

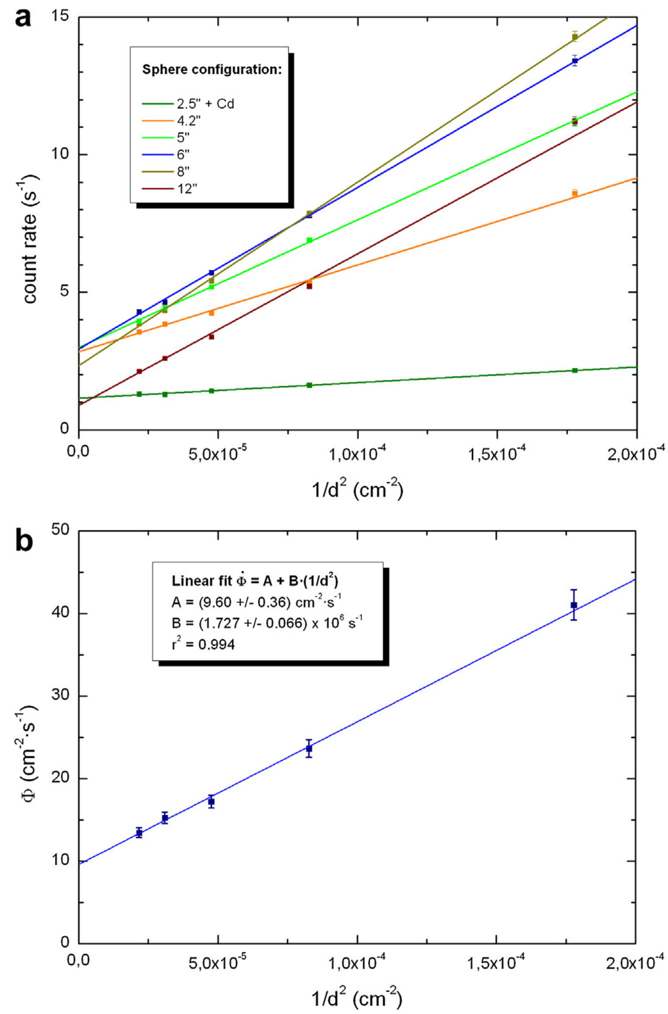

Fig. 3. (a) Linear fits of full count rates against $1/d^2$ for some representative spheres (2.5″ + Cd, 4.2″, 5″, 6″, 8″ and 12″); (b) Plot and linear fit of measured full neutron fluence rates $\dot{\Phi}_d$ against $1/d^2$.

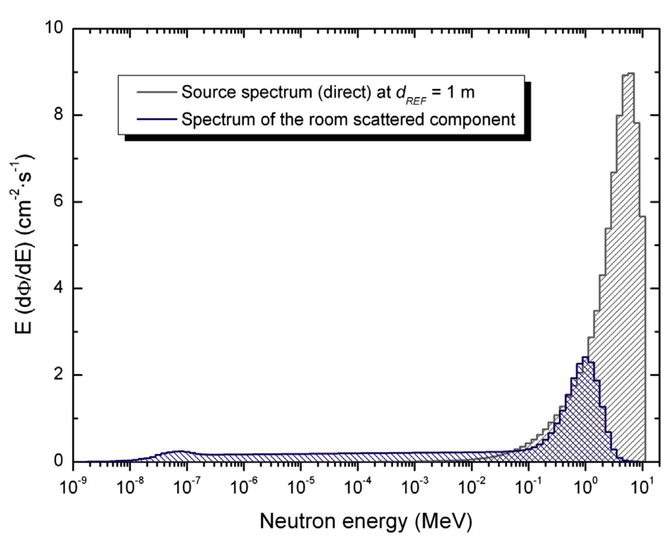

Fig. 4. Direct (un-scattered) neutron spectrum evaluated at d_{REF} and scattered neutron spectrum.

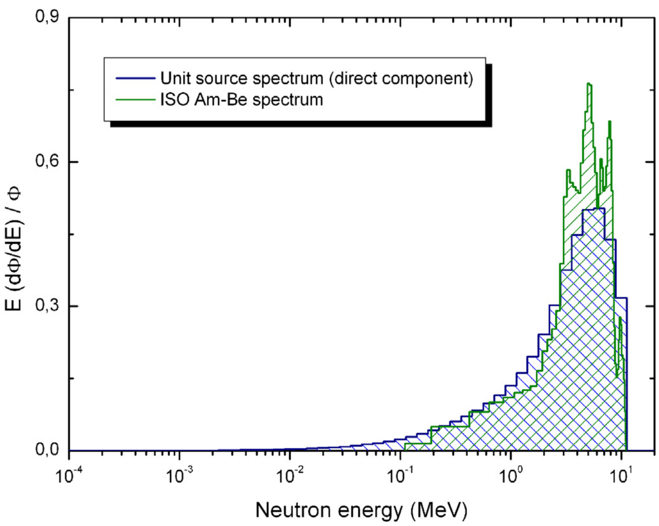

Fig. 5. Measured and ISO-8529 unit direct un-scattered neutron spectra emitted from the ^{241}Am-Be source.

include the combination of counting uncertainties, of uncertainties of the parameters obtained from least-squares fits, of the response function calculation uncertainties and of other sources of uncertainty, like detector response variability and calibration factor uncertainty. The value obtained of source intensity is in fairly satisfactory agreement with that estimated from the nominal ^{241}Am source activity (1 Ci = 3.7×10^{10} Bq) and the measured neutron yield per unit activity, 7.0×10^{-5} s^{-1} Bq^{-1} (Knoll, 2000), that results in a neutron yield of 2.6×10^{6} s^{-1}. Similarly, unfolding c^{i}_{∞} leads to the spectrum of the scattered neutron component and its corresponding fluence rate, $\dot{\Phi}^{s} = (7.43 \pm 0.55)$ cm^{-2} s^{-1}. In the constant scattering approximation, this component is uniform throughout the irradiation room. The value obtained is not far from the roughly estimated value $\dot{\Phi}_{\infty}$, as described above.

Fig. 4 shows the direct neutron spectrum at d_{REF} and the scattered neutron spectrum. One relevant feature of the scattered spectrum is the presence of a peak at relatively high energy ($\approx$1 MeV), which is probably due to the fact that many neutrons may reach the detector after a very small number of single interactions, not sufficient to become thermal, because of the very reduced dimensions of the irradiation room.

Finally, Fig. 5 displays a comparison between the measured un-scattered neutron spectrum directly emitted from the ^{241}Am-Be source of the IPHC irradiation facility and that given by the ISO-8529 standard, both normalised to the total fluence rate (unit spectra). As shown in this figure, there is a reasonable coincidence between the two spectra above 100 keV if we take into account the limited energy resolution of the BSS. For energies below 100 keV there is a possible discrepancy between the unfolded spectrum and the ISO spectrum, especially for very low energies where the ISO spectrum is set to 0. Further experimentation with higher precision would be needed to ascertain these possible discrepancies.

4. Conclusions

The IPHC neutron irradiation facility, which is based on an ^{241}Am-Be radionuclide source, was fully characterized by means of a Bonner sphere spectrometer and MCNPX simulations. It has been demonstrated, by assuming constant scattering and negligible air-attenuation within the irradiation room, that the fast neutron component (between 10 keV and 1 MeV) is originally emitted from the ^{241}Am-Be source and decreases with distance (d) according to the $1/d^2$ law. The estimated un-scattered neutron spectrum emitted from the ^{241}Am-Be source is in agreement with that given for the ISO-8529 standard for energies above 100 keV, while further experimentation would be needed to ascertain possible discrepancies appearing for very low energies, where the ISO spectrum is set to 0, but a small contribution, decreasing for decreasing energies, appears in the unfolded spectrum.

Acknowledgements

This work was partially funded by the convention between IN2P3 (Institut National de Physique Nucléaire et de Physique des Particules, France) and MICINN (Ministerio de Ciencia e Innovación, Spain) FPA2008-04155-E, by MICINN project FIS2009-10634, and by the Catalan Research Management Agency (AGAUR) project 2009SGR-122.

References

Abou-Khalil, R., Michielsen, N., Della-Negra, S., Nourreddine, A., Baussan, E., 2009. Electric charge spectrum of recoiling ^{218}Po. Radiat. Meas. 44, 1055–1057.
Amgarou, K., Bedogni, R., Domingo, C., Esposito, A., Gentile, A., Carinci, G., Russo, S., 2011. Measurement of the neutron fields produced by a 62 MeV proton beam on a PMMA phantom using extended range Bonner sphere spectrometers. Nucl. Instr. Meth. A 654, 399–405.
Bakali, M., 2001. Ph.D. thesis, Univ. Autònoma de Barcelona. (in Spanish).
Bedogni, R., Esposito, A., Domingo, C., Fernández, F., Garcia, M.J., Angelone, M., 2007a. Performance of the UAB and the INFN-LNF Bonner sphere spectrometers in quasi monoenergetic neutron fields. Radiat. Prot. Dosim. 126, 361–365.
Bedogni, R., Domingo, C., Esposito, A., Fernández, F., 2007b. FRUIT: an operational tool for multisphere neutron spectrometry in workplaces. Nucl. Instr. Meth. A 580, 1301–1309.
Bedogni, R., Domingo, C., Esposito, A., Chiti, M., García-Fusté, M.J., Lovestam, G., 2010. Testing Bonner sphere spectrometers in the JRC-IRMM mono-energetic neutron beams. Nucl. Instr. Meth. A 620, 391–396.
Bramblett, R.L., Ewing, R.I., Bonner, T.W., 1960. A new type of neutron spectrometer. Nucl. Instr. Meth. 9, 1–12.
Domingo, C., Amgarou, K., García-Fusté, M.J., Garcia-Orellana, J., Morales, E., Bouassoule, T., Castelo, J., Fernández, F., 2009. Neutron dosimetric studies of density/moisture gauge operators during transport and usage. Radiat. Meas. 44, 1002–1005.
Dziri, S., Nourreddine, A., Sellam, A., Pape, A., Baussan, E., 2012. Simulation approach to coincidence summing in γ-ray image spectrometry. Appl. Radiat. Isot. 70, 1141–1144.
Esposito, A., Bedogni, R., Domingo, C., García, M.J., Amgarou, K., 2010. Measurements of leakage neutron spectra from a high-energy accumulation ring using extended range Bonner sphere spectrometers. Radiat. Meas. 45, 1522–1525.
Fernández, F., Bakali, M., Tomás, M., Muller, H., Pochat, J.L., 2004. Neutron measurements in the Vandellòs II nuclear power plant with a Bonner sphere system. Radiat. Prot. Dosim. 110, 517–521.
Fernández, F., Amgarou, K., Domingo, C., García, M.J., Nourreddine, A., Mouhssine, D., Belafrites, A., Ribaud, I., 2005. A joint UAB-IReS-IPNO neutron comparison exercise with nuclear track detectors. Radiat. Meas. 40, 601–607.
Fernández, F., Bouassoule, T., Amgarou, K., Domingo, C., Garcia, M.J., Lacoste, V., Gressier, V., Muller, H., 2007a. Monte Carlo calculations and validation of a gold-foil based Bonner sphere system. Radiat. Prot. Dosim. 126, 366–370.
Fernández, F., Amgarou, K., Domingo, C., García, M.J., Quincoces, G., Martí-Climent, J.M., Méndez, R., Barquero, R., 2007b. Neutron spectrometry in a PET cyclotron with a Bonner sphere system. Radiat. Prot. Dosim. 126, 371–375.
Fernández, F., Domingo, C., Amgarou, K., Bouassoule, T., García, M.J., 2007c. Neutron measurements in Spanish nuclear power plants with a Bonner sphere spectrometer system. Radiat. Prot. Dosim. 126, 355–360.
Gressier, V., Lacoste, V., Lebreton, L., Muller, H., Pelcot, G., Bakali, M., Fernández, F., Tómas, M., Roberts, N.J., Thomas, D.J., Reginatto, M., Wiegel, B., Wittstock, J., 2004. Characterisation of the IRSN CANEL/T400 facility producing realistic neutron fields for calibration and test purposes. Radiat. Prot. Dosim. 110, 523–527.
International Commission on Radiological Protection (ICRP), 1997. Conversion Coefficients for Use in Radiological Protection against External Radiation. publication 75. Pergamon Press.
International Organisation for Standardisation (ISO), 1989. Neutron Reference Radiations for Calibrating Neutron-measuring Devices Used for Radiation Protection Purposes and for Determining Their Response as a Function of Neutron Energy. ISO-8529 standard.
Knoll, G.F., 2000. Radiation Detection and Measurement, third ed. John Wiley & Sons, p. 22.
Lacoste, V., Gressier, V., Pochat, J.-L., Fernandez, F., Bakali, M., Bouassoule, T., 2004. Characterization of Bonner sphere systems at mono-energetic and thermal neutron fields. Radiat. Prot. Dosim. 110, 529–532.

Mouhssine, D., Nourreddine, A., Nachab, A., Fernandez, F., Domingo, C., Muller, H., Amgarou, K., Pape, A., Raiser, D., 2005. Calibration factor for estimating personal dose equivalent with imaging plates. Radiat. Meas. 40, 607–611.

Ngachin, M., Garavaglia, M., Giovani, C., Kwato Njock, M.G., Nourreddine, A., 2008. Radioactivity level and soil radon measurement of a volcanic area in Cameroon. J. Environ. Radioact. 99, 1056–1060.

Ouziane, S., Amokrane, A., Toumert, I., Nourreddine, A., 2010. ^{4}He-induced L X-ray production cross sections in Pt and Bi. Nucl. Instr. Meth. B 267, 1764–1766.

Reginatto, M., 2010. Overview of spectral unfolding techniques and uncertainty estimation. Radiat. Meas. 45, 1323–1329.

Waters, L.S. (Ed.), 2002. MCNPXTM Users Manual, ECI, Version 2.4.0. Los Alamos National Laboratory. report LA-CP-02-408.